

Published in final edited form as:

Dev Biol. 2012 March 1; 363(1): 234–246. doi:10.1016/j.ydbio.2011.12.034.

Tbx20 regulation of cardiac cell proliferation and lineage specialization during embryonic and fetal development *in vivo*

Santanu Chakraborty and Katherine E. Yutzey*

The Heart Institute, Cincinnati Children's Medical Center, Cincinnati, OH 45229

Abstract

TBX20 gain-of-function mutations in humans are associated with congenital heart malformations and myocardial defects. However the effects of increased *Tbx20* function during cardiac chamber development and maturation have not been reported previously. *CAG-CAT-Tbx20* transgenic mice were generated for Cre-dependent induction of *Tbx20* in myocardial lineages in the developing heart. β MHCCre-mediated overexpression of *Tbx20* in fetal ventricular cardiomyocytes results in increased thickness of compact myocardium, induction of cardiomyocyte proliferation, and increased expression of *Bmp10* and pSmad1/5/8 at embryonic day (E) 14.5. β MHCCre-mediated *Tbx20* overexpression also leads to increased expression of cardiac conduction system (CCS) genes *Tbx5*, *Cx40*, and *Cx43* throughout the ventricular myocardium. In contrast, *Nkx2.5*Cre mediated overexpression of *Tbx20* in the embryonic heart results in reduced cardiomyocyte proliferation, increased expression of a cell cycle inhibitor, p21^{CIP1}, and decreased expression of *Tbx2*, *Tbx5*, and *N-myc1* at E9.5, concomitant with decreased phospho-ERK1/2 expression. Together, these analyses demonstrate that *Tbx20* differentially regulates cell proliferation and cardiac lineage specification in embryonic versus fetal cardiomyocytes. Induction of pSmad1/5/8 at E14.5 and inhibition of dpERK expression at E9.5 are consistent with selective *Tbx20* regulation of these pathways in association with stage-specific effects on cardiomyocyte proliferation. Together, these *in vivo* data support distinct functions for *Tbx20* in regulation of cardiomyocyte lineage maturation and cell proliferation at embryonic and fetal stages of heart development.

Keywords

T-box transcription factors; *Tbx20*; cardiomyocyte proliferation; phospho-ERK 1/2; bone morphogenetic protein 10; phospho-Smad1/5/8

Introduction

T-box (*Tbx*) transcription factors are critical regulators of heart development, and mutations in several *TBX* genes in humans are associated with congenital cardiac anomalies (Plageman and Yutzey, 2005; Stennard and Harvey, 2005). *Tbx20*, a member of the *Tbx1* subfamily of T-box genes, is expressed in multiple organs, including the developing heart (Plageman and

© 2012 Elsevier Inc. All rights reserved.

*Address Correspondence to: Katherine E. Yutzey, The Heart Institute, Division of Molecular Cardiovascular Biology, Cincinnati Children's Medical Center MLC 7020, 240 Albert Sabin Way, Cincinnati, OH 45229, Tel: 513-636-8340; Fax: 513-636-5958, katherine.yutzey@cchmc.org .

Publisher's Disclaimer: This is a PDF file of an unedited manuscript that has been accepted for publication. As a service to our customers we are providing this early version of the manuscript. The manuscript will undergo copyediting, typesetting, and review of the resulting proof before it is published in its final citable form. Please note that during the production process errors may be discovered which could affect the content, and all legal disclaimers that apply to the journal pertain.

Yutzey, 2004; Stennard et al., 2003; Takeuchi et al., 2003). Mutations in human *TBX20* that result in gain or loss of protein function are associated with a wide array of cardiac malformations, including septal defects, defects in valvulogenesis, and cardiomyopathy (Kirk et al., 2007; Posch et al., 2010). In mice, systemic loss of *Tbx20* results in lethality by embryonic day (E) 10.5, associated with reduced myocardial proliferation and inhibition of chamber differentiation (Cai et al., 2005; Singh et al., 2005; Stennard et al., 2005; Takeuchi et al., 2005). Direct downstream target genes of *Tbx20* in the primitive myocardium include *Tbx2* and *N-myc1*, that function to regulate cardiomyocyte proliferation (Cai et al., 2005). In adult mice, heterozygous loss of *Tbx20* leads to dilated cardiomyopathy (Stennard et al., 2005) and conditional homozygous loss of *Tbx20* in cardiomyocytes results in severe cardiomyopathy with associated arrhythmias and death (Shen et al., 2011). However, the specific functions of *Tbx20* in the developing myocardium after the initial stages of heart chamber specification have not been defined *in vivo*.

During embryonic and fetal development, multiple regulatory pathways control differential rates of cardiomyocyte proliferation necessary for proper cardiac chamber morphogenesis and function (Sedmera and Thompson, 2011). During embryonic stages of chamber morphogenesis (mouse E9.5-E11.5), Neuregulin1 (*Nrg1*), an endocardium-derived mitogen, promotes the initiation of trabecular myocardial outgrowth and cardiomyocyte proliferation via ErbB receptors and ERK/MAP-kinase activation (Lai et al., 2010; Stennard et al., 2005; Woldeyesus et al., 1999). During formation of the ventricular compact layer at fetal stages (E12.5-E17.5), *Bmp10* signaling through pSmad1/5/8 activation is required for ventricular cardiomyocyte proliferation, and cardiomyocyte-specific loss of *Smad4*, necessary for BMP signaling, leads to myocardial hypoplasia with decreased expression of *N-myc1*, *cyclinD1*, and *cyclinD2* (Chen et al., 2004; Song et al., 2007). A critical difference in regulation of embryonic and fetal myocardial proliferation is the presence of the epicardium, which is a source of several mitogens, including IGF2 and FGF9, that promote fetal ventricular compact layer cell proliferation (Lavine et al., 2005; Li et al., 2011; Sucov et al., 2009). Thus, multiple signaling pathways have been implicated in the regulation of cardiomyocyte proliferation in the developing heart. However, less is known about the contributions of specific transcription factors or the mechanisms of integration of these pathways in the control of differential rates of proliferation during cardiac organogenesis.

Transgenic mice were generated with Cre-dependent overexpression of *Tbx20* in embryonic or fetal cardiomyocytes. Induction of *Tbx20* expression in the fetal ventricles (E12.5-E17.5) with β MHCCre results in increased cell proliferation, with increased expression of *N-myc1*, *Bmp10*, and pSmad1/5/8, as well as increased expression of conduction system markers *Tbx5*, *Cx40*, and *Cx43* throughout the ventricular myocardium. In contrast, induction of *Tbx20* expression in the embryonic heart (E9.5) with *Nkx2.5*Cre results in a small heart with decreased cell proliferation, apparently normal induction of chamber maturation gene expression, and attenuated activation of ERK1/2 MAPK. Thus, *Tbx20* overexpression has opposite effects on cardiomyocyte cell proliferation and lineage maturation in embryonic and fetal cardiomyocytes that is associated with differential regulation of ERK1/2 and Smad1/5/8 signaling *in vivo*.

Materials and methods

Generation of transgenic mice

The Cre-responsive transgene *CAG-CAT-Tbx20* (*CC-Tbx20*) was constructed by modification of the CAG-CAT-Z construct, which contains a CMV enhancer and chicken β -actin gene (CAG) promoter, linked to the *chloramphenicol acetyltransferase* (CAT) gene, flanked by *loxP* sites (Araki et al., 1995). The full-length murine *Tbx20* coding sequence was isolated from *pAC-CMV-Tbx20* (Plageman and Yutzey, 2004) and inserted into the BamHI

site of CAG-CAT-Z in place of *LacZ* (Araki et al., 1995). The *Tbx20* transgene consists of the *Tbx20a* isoform that includes both transactivation and transrepression domains (Stennard et al., 2003). This isoform is preferentially expressed in the cardiac OFT region at E9.5-E12.5, although expression is detected throughout the primitive heart tube at E9.5-E10.5 (Takeuchi et al., 2005). Successful insertion of the full-length murine *Tbx20* coding sequence was verified by direct sequencing of the *CC-Tbx20* transgenic construct. The purified linearized construct was introduced by pronuclear microinjection of fertilized blastocysts of FVBN mice. Transgenic founder lines were validated by genotyping using *CAG-CAT* (5'-TCA CTG CAT TCT AGT TGT GGT TTG-3') and *Tbx20* (5'-TTG GAC TCA GGA TCC ACT CC-3') specific primers. Transgene expression in multiple organs was confirmed by the presence of CAT protein detected by CAT-ELISA assay (Roche, #11363727001, used as per manufacturer's protocols) in two independent founder lines. The founder line with robust expression of CAT protein in the heart was used for all subsequent *in vivo* transgenic analyses. Female *CAG-CAT-Tbx20* mice were bred with β *MHCCre* (Parsons et al., 2004) or *Nkx2.5Cre* (Moses et al., 2001) males to generate double transgenic embryos, neonates, and adult offspring. Timed matings were established, with the morning of an observed copulation plug set at E0.5. All studies were performed on cohorts of β *MHCCre*;*CC-Tbx20*, or *Nkx2.5Cre*;*CC-Tbx20*, double transgenic (DTG) animals compared to single transgenic (STG) *CC-Tbx20* littermate controls. Genotyping for β *MHCCre* (Parsons et al., 2004) and *Nkx2.5Cre* (Moses et al., 2001) was performed as described previously by PCR of genomic DNA isolated from embryonic yolk sacs or 3 weeks postnatal tail clips. All experiments involving animals were carried out with experimental protocols and procedures reviewed and approved by the Cincinnati Children's Medical Center Institutional Biosafety Committee and Institutional Animal Care and Use Committee.

In situ hybridization (ISH) and immunohistochemistry

Whole embryos isolated at E9.5 or E14.5 and hearts isolated at E17.5 were collected and processed for either *in situ* hybridization (ISH) or immunohistochemistry as previously described (Chakraborty et al., 2008; Chakraborty et al., 2010; Lincoln et al., 2006). The generation of antisense RNA probes and ISH were performed as previously described (Chakraborty et al., 2008). The plasmids for generation of *Bmp10* (Chen et al., 2004), *Nppa*, *Smpx*, *Tbx2*, *Cx40*, *Cx43* (Christoffels et al., 2004), *Tbx5* (Takeuchi et al., 2005), *N-myc1* (Cai et al., 2005) and *MLC2v* (Liberatore et al., 2000) antisense RNA probes were used as previously described. For histology, tissues were deparaffinized and dehydrated through a graded ethanol series, followed by staining with Hematoxylin and Eosin (H&E) as previously described (Hinton et al., 2006).

The following antibodies were used for immunofluorescence (IF) and/or colorimetric immunohistochemistry with diaminobenzidine (DAB) detection: Phospho-Histone H3 (pHH3) (1:100; Millipore, 06-570), MF20 (1:200; Developmental Studies Hybridoma Bank, University of Iowa), pSmad1/5/8 (1:100; Millipore, AB3848), *Tbx20* (1:100; Orbigen, PAB 11248), p21^{CIP1} (BD Pharmigen, 556430), Diphosphorylated ERK-1/2 (dpERK) (1:10000; Sigma, M 8159) and Twist1 (1:50; Santa Cruz, SC 81417). IF and colorimetric detection methods were performed essentially as previously described (Chakraborty et al., 2010). For IF, Alexa Fluor 488 (green)- and/or 568 (red)-conjugated goat anti-rabbit or goat anti-mouse secondary antibodies (Molecular Probes, 1:100) were used with ToPro3 (Molecular Probes, 1:1000) for visualization of nuclei. Fluorescence was visualized using a Zeiss LSM 510 confocal microscope and LSM version 3.2 SP2 software. For colorimetric immunohistochemistry, primary antibodies were detected using the Ultra-sensitive ABC rabbit (anti-*Tbx20*) or mouse (anti-Twist1, -dpERK) IgG staining kit according to manufacturer's suggested guidelines (Thermo Scientific, 32054 and 32052). Antibody

staining was visualized using the metal enhanced DAB substrate staining kit (Thermo Scientific, 34065).

β -galactosidase (β -gal) detection

β -gal expression was analyzed in whole (E12.5) and bisected hearts (E14.5 and E17.5) using X-gal detection of β -gal activity as previously described (Lincoln et al., 2004; Searcy et al., 1998). For histology, X-gal stained embryos (E12.5) or bisected hearts (E14.5 and E17.5) were dehydrated through a graded isopropanol/PBT series and paraffin wax embedded. Ten μ m sections were cut, deparaffinized in two changes in xylene for 5 min each and mounted in Cytoseal 60 (Richard-Allen Scientific) for microscopy and imaging.

RNA isolation and real-time quantitative RT-PCR (qRT-PCR)

Hearts were isolated from E9.5 embryos, and ventricles were isolated from E14.5 and E18.5 embryos generated from multiple matings of *CC-Tbx20* females and *Cre* (β MHC or *Nkx2.5*) males. After PCR genotyping, tissue from 4-6 early (E9.5 and E14.5) or 2-3 late (E18.5) embryos was pooled for RNA isolation, and real time qRT-PCR was performed as previously described (Chakraborty et al., 2008; Chakraborty et al., 2010). Forward and reverse primer sequences designed for qRT-PCR are *Nppa* (5'-GTG AGC AGA CTG AGG AAG CA-3' and 5'-TGC TTT TCA AGA GGG CAG AT-3'); *Tbx5* (5'-ATG GTC CGT AAC TGG CAA AG-3' and 5'-TTT CGT CTG CTT TCA CGA TG-3'); *Cx40* (5'-CCT GGA TAC CCT GCA TGT CT-3' and 5'-GCT GTC GGA TCT TCT TC AG-3'); *Cx43* (5'-GAA CAC GGC AAG GTG AAG AT-3' and 5'-GA CGA GAG ACA CCA AGG AC-3'); *N-myc1* (5'-CAG CTG CAC CGC GTC CAC CA-3' and 5'-CAT GCA GTC CTG AAG GAT GA-3'); *Bmp10* (5'-ACC AGA CGT TGG CAA AAG TCA GGC-3' and 5'-GAT GAT CCA GGA GTC CCA CCC AAT-3'); *Tbx2* (5'-TGA CAA GCA TGG CTT TAC CA-3' and 5'-GTA GGC AGT GAC AGC GAT GA-3'). The primer sequences for *p21^{CIP1}*, *p27^{KIP1}* (Evans-Anderson et al., 2008), *Cyclin A2* (Gurtner et al., 2008), *Cyclin D1* (Kroger et al., 2007), *Cyclin E1* (Xue et al., 2010), *Mlc2v*, *Smpx* (Lai et al., 2010) and *Nrg1* (Kato et al., 2010) qRT-PCR were described previously. All the amplification reactions were performed with 34 cycles of 94° C for 30 seconds; 55° C for 45 seconds; and 72° C for 30 seconds. A standard curve was generated for each primer pair using E9.5 or E14.5 whole embryo-derived cDNA, and all the values were normalized to ribosomal protein *L7* expression (Hemmerich et al., 1993). For each gene, normalized expression in DTG tissue is set to 1 and then the fold-change is calculated for corresponding DTG samples. qRT-PCR results represent three independent samples (biological 3X) performed in triplicate (technical 3X). Statistical significance of observed differences was determined by Student's *t*-test ($p < 0.01$).

Protein isolation and Western blotting

Protein lysates were isolated from E9.5, E12.5 E14.5, and E17.5 whole hearts using ice-cold CelLytic MT tissue lysis buffer (Sigma), containing protease inhibitor mixture (Pierce) and phosphatase inhibitor (Pierce) according to manufacturer's guidelines. After PCR genotyping, hearts from 6-8 early (E9.5 and E12.5) or 2-3 late (E14.5 and E17.5) embryos were pooled for total protein isolation, and Western blots were performed as described previously (Chakraborty et al., 2010). Immunoblots were developed using chemifluorescent detection with the Vistra ECF reagent (Amersham Biosciences) and scanned using a Storm 860 phosphorimager (Amersham Biosciences). Signal intensities were quantified with ImageQuant 5.0 software (GE Healthcare). *Tbx20* (1:500; Orbigen, PAB 11248), pSmad 1/5/8 (1:500; Millipore, AB3848), ERK (1:1000; Cell Signaling, 9102) and p-ERK (1:1000; Cell Signaling, 9101) primary antibodies were used for immunoblot analysis. GAPDH (1:4000; Santa Cruz) antibody reactivity was used as a loading control. Statistical significance was determined by Student's *t*-test ($p < 0.05$).

Quantitative analyses of cell density, ventricular wall thickness, and cell proliferation

The average number of cell nuclei per area of compact myocardium and left ventricular wall thickness were determined using ImageJ software (NIH). Measurements were taken on H&E stained photomicrographs of 5-6 tissue sections per heart from at least 4 hearts per genotype. Proliferative indices of cardiomyocytes were calculated as the total number of pHH3 nuclei in MF20-positive cardiomyocytes/total number of nuclei in MF20-positive cardiomyocytes. Likewise, the number of Tbx20 nuclei in MF20-positive cardiomyocytes/total number of nuclei in MF20-positive cardiomyocytes was determined as a quantitative measure of Tbx20 overexpression in *Nkx2.5Cre* mice. At least 250 cell nuclei were counted from each heart section showing LV or RV chamber myocardium. Proliferative indices and total cell counts were calculated in multiple sections of 4-6 hearts of each genotype using ImageJ software (NIH). All the average measurements are reported with \pm standard error of mean (SEM) and statistical significance was determined by Student's *t*-test ($p < 0.05$).

Chromatin immunoprecipitation (ChIP) assay

Direct Tbx20 binding to chromosomal DNA *in vivo* was evaluated in individual mouse hearts dissected from β MHCCre;*CC-Tbx20* (DTG) and littermate *CC-Tbx20* (STG) controls at E17.5. DNA/protein complexes were cross-linked for 10 min in formaldehyde (Sigma) at a final concentration of 1%. The fixed cells were lysed and sonicated twice for 5 s each output 5 (Virsonic 60; Virtis) and a 2 min refractory period. For immunoprecipitation, cell lysates were incubated with an antibody against Tbx20 (5 μ g; Orbigen) and incubated overnight at 4 $^{\circ}$ C. Immunoprecipitation with normal rabbit IgG was used as a negative control. ChIP assays were performed according to the manufacturer's instructions (EZChIP, Upstate), with the exception that protein A-agarose beads were used. The immunoprecipitated and input DNA were subjected to quantitative PCR using SYBR Green PCR reagents and MJ Research Opticon 2 machine. P-4030 and P-4330 primers were used to amplify the *N-myc1* intron 1 promoter region, and P-813 and P-573 primers were used to amplify the *Tbx2* promoter region as previously described (Cai et al., 2005). Fold enrichment relative to IgG antibody control (negative control) was calculated using the comparative C_T method ($\Delta\Delta C_T$) as described previously (n = 3) (Mandel et al., 2010; Sengupta et al., 2011). Statistical significance was determined by Student's *t*-test ($p < 0.05$).

Results

β MHCCre-mediated Tbx20 overexpression in differentiated cardiomyocytes results in thickening of ventricular myocardium

In order to determine the effects of Tbx20 gain-of-function in the developing heart, mice were generated to express a Cre-inducible *CAG-CAT-Tbx20* (*CC-Tbx20*) transgene (Fig. 1A). The *CAG-CAT-Tbx20* transgene consists of a *CAG* regulatory element, that includes a CMV enhancer/ β -actin promoter driving the ubiquitous expression of *CAT*, flanked by *loxP* sites, linked to *Tbx20*. *CAT* expression from the transgene was detected by ELISA in multiple organs (heart, brain and lung) in founder lines (data not shown). In the presence of Cre, the floxed *CAT* gene is deleted and Tbx20 is expressed. Therefore, conditional overexpression of Tbx20 is achieved in both a spatially and temporally regulated manner in double transgenic (DTG) animals expressing Cre from β MHC or *Nkx2.5* promoters in the presence of the *CC-Tbx20* transgene.

In order to achieve increased Tbx20 expression in differentiated cardiomyocytes, *CC-Tbx20* transgenic mice were mated with β MHCCre mice (Parsons et al., 2004). β MHCCre-mediated overexpression of Tbx20 was confirmed by Tbx20 specific antibody staining in E14.5 chamber myocardium. β MHCCre activity in the developing murine heart is apparent throughout the myocardium at E12.5, E14.5, and E17.5 as indicated by Rosa26R reporter

expression analysis (Supplemental Fig. S1). Tbx20 immunoreactivity, is increased both in the interventricular septum (IVS in Fig. 1C) and left ventricular (LV in Fig. 1E) myocardium of the β MHCCre;CC-Tbx20 double transgenic (DTG) animals compared to the littermate CC-Tbx20 single transgenic (STG) control (Fig. 1B, D). Tbx20 protein localization, as detected by immunostaining, is predominantly nuclear in both STG and DTG animals. Quantitative Western blot analysis reveals increased expression of Tbx20 in β MHCCre;CC-Tbx20 DTG hearts beginning at E12.5, with an approximately 3-fold increase in Tbx20 protein expression at E14.5 and E17.5, compared to endogenous Tbx20 levels (Fig. 1F, G). During development and after birth, β MHCCre;CC-Tbx20 DTG animals were obtained at the expected Mendelian ratio, and no embryonic or adult morbidity or mortality was observed (Table 1).

Histological analysis of E14.5 DTG chamber myocardium overexpressing Tbx20 reveals fewer trabeculae in the ventricular myocardium (asterisks, Fig. 1H, I) and an increase in the average number of nuclei per area of the compact myocardium (Fig. 1J), compared to littermate STG controls. In addition, the thickness of the compact myocardium also is significantly increased in the E17.5 DTG hearts as compared to littermate controls (Fig. 1K-M). Thus, β MHCCre-mediated Tbx20 overexpression results in increased cell number and thickness of the developing compact myocardium at E14.5-E17.5.

β MHCCre-mediated Tbx20 overexpression promotes cardiomyocyte proliferation with increased binding to the *N-myc1* promoter region in β MHCCre;CC-Tbx20 fetal hearts *in vivo*

Cardiomyocyte proliferation was examined in the hearts of β MHCCre;CC-Tbx20 DTG embryos relative to littermate controls. Consistent with the increased number of cells in ventricular myocardium with Tbx20 overexpression, the number of phospho-histone H3 (pHH3) positive nuclei in MF20 positive cardiomyocytes is increased in DTG embryos, compared to littermate STG controls at E14.5 (arrowheads, Fig. 2A, B). Quantitation of these results demonstrates that 20.7% of the nuclei of MF20 positive cardiomyocytes are also positive for pHH3 in DTG myocardium overexpressing Tbx20, compared to 9.3% of the cardiomyocyte nuclei in STG littermates (Fig. 2C) at E14.5. Thus increased Tbx20 expression promotes myocardial cell proliferation at E14.5.

N-myc1 is a downstream target gene of Tbx20 in cardiomyocytes and is a positive regulator of cellular proliferation (Cai et al., 2005; Davis and Bradley, 1993). *N-myc1* expression is increased in β MHCCre;CC-Tbx20 DTG myocardium with Tbx20 overexpression as detected by ISH (arrows, Fig. 2D, E). Expression of *N-myc1* mRNA is increased by 3.8-fold in E14.5 DTG hearts overexpressing Tbx20, relative to controls, as determined by qRT-PCR (Fig. 2F). In cardiomyocytes, Tbx20 promotes cell proliferation through activation and binding to regulatory elements of *N-myc1* and *Tbx2* genes (Cai et al., 2005). Therefore, ChIP assays were performed to determine if Tbx20 binding to the promoter region of *N-myc1* is increased in association with increased gene expression in fetal cardiomyocytes overexpressing Tbx20. In E17.5 DTG hearts, Tbx20 binds to the promoter region of *N-myc1* with 14.5-fold enrichment over IgG controls, compared to 3-fold enrichment in STG littermates (Fig. 2G). Interestingly, no difference in Tbx20 binding to the *Tbx2* promoter region was observed by ChIP analysis, consistent with no observed change in gene expression in DTG versus STG hearts (data not shown). Together, these data suggest that Tbx20 directly binds and induces *N-myc1* expression while also promoting cardiomyocyte proliferation in β MHCCre;CC-Tbx20 hearts *in vivo*.

Bmp10* expression and pSmad1/5/8 signaling is increased in differentiated fetal cardiomyocytes overexpressing *Tbx20

Cardiomyocyte proliferation during heart chamber maturation is dependent on *Bmp10* (Chen et al., 2004). Therefore, *Bmp10* mRNA expression was evaluated in DTG hearts overexpressing *Tbx20*. Expression of *Bmp10* transcripts is increased in DTG myocardium overexpressing *Tbx20*, as detected by ISH, compared to littermate control (Fig. 3A, B). Likewise, *Bmp10* mRNA expression is increased by 2.9-fold in E14.5 DTG hearts relative to littermate STG controls, as detected by qRT-PCR (Fig. 3C). Increased BMP signaling in the heart also is apparent as an increase in the number of phospho-Smad1/5/8 (pSmad1/5/8) positive nuclei at E14.5 and E17.5, compared to STG controls (Fig. 3D-G). Increased pSmad1/5/8 positive nuclei are apparent in MF20-positive and -negative cells in the DTG ventricles, indicative of increased BMP signaling in multiple cell types. Quantitation of pSmad1/5/8 protein expression by Western blot demonstrates a 2.1-fold increase in total pSmad1/5/8 protein levels in E14.5 DTG hearts, compared to littermate STG controls (Fig. 3H-I). In contrast, pSmad1/5/8 expression levels were unchanged in *Nkx2.5Cre;CC-Tbx20* embryonic ventricular cardiomyocytes (E9.5) compared to littermate STG controls (Supplemental Fig. S2A-D). Thus, *Tbx20* promotes *Bmp10* expression and pSmad1/5/8 signaling specifically associated with increased cell proliferation of fetal, but not embryonic, cardiomyocytes.

β MHCCre-mediated *Tbx20* overexpression represses *Tbx2*, while promoting *Tbx5*, connexin 40 (*Cx40*) and connexin 43 (*Cx43*), expression in ventricular cardiomyocytes

Localized expression of *Tbx2* and *Tbx5* was examined in hearts with *Tbx20* overexpression. In β MHCCre;*CC-Tbx20* DTG hearts, the expression of *Tbx2* is reduced in the AVC myocardium at E14.5, compared to normal expression in the littermate control heart, as detected by ISH (Fig. 4A, B). In contrast, *Tbx5* expression is induced throughout the septum (IVS) and in the ventricles in DTG hearts compared to localized expression in the littermate control heart at E18.5 (Fig. 4C-F). Consistent with previous reports (Hatcher et al., 2000), *Tbx5* expression is detected at the epicardial surface of E18.5 STG hearts, and decreased epicardial expression of *Tbx5* was noted in multiple E18.5 DTG hearts (Fig. 4E, F). Thus *Tbx20* overexpression leads to decreased *Tbx2* expression in the AVC and increased expression of *Tbx5* throughout the developing ventricles, but not epicardium, of β MHCCre;*CC-Tbx20* DTG fetuses *in vivo*.

Gene expression of T-box downstream target genes *Cx40* and *Cx43* expressed in the cardiac conduction system (CCS) as examined in β MHCCre;*CC-Tbx20* DTG hearts at E18.5 (Christoffels et al., 2010). At this stage, *Cx40* expression is normally restricted to the ventricular conduction tissues, and *Cx43* is expressed in the trabecular and, to a lesser extent, the compact myocardium (Coppin et al., 2003). In β MHCCre;*CC-Tbx20* DTG hearts, the expression of both the *Cx40* and *Cx43* transcripts is increased throughout the full thickness of the ventricular walls, including the interventricular septum (Fig. 4G-N). In contrast, expression of *Nppa*, which is regulated by multiple Tbx factors including *Tbx5* and *Tbx2* (Habets et al., 2002), is apparently unaltered in the DTG trabecular myocardium, compared to a littermate control heart (Fig. 4O, P). Gene expression changes detected by ISH were further confirmed by qRT-PCR (Fig. 4Q). Since altered expression of Connexin genes would be expected to affect the CCS, AV conduction system function was evaluated in adult hearts overexpressing *Tbx20* by surface electrocardiography (ECG). However no significant changes in AV conduction system amplitudes or intervals were detected, at least at the baseline level, in *Tbx20* DTG adult animals compared to littermate controls (data not shown). Thus *Tbx20* overexpression in ventricular cardiomyocytes at fetal stages results in decreased expression of *Tbx2* and increased expression of *Tbx5*, with widespread increased expression of Connexins (*Cx40* and *Cx43*) beyond the CCS.

Nkx2.5Cre-mediated Tbx20 overexpression results in a smaller heart with decreased expression of *Tbx5*, but apparently normal expression levels of chamber maturation genes

Nkx2.5Cre;CC-Tbx20 DTG mice were generated in order to determine effects of increased Tbx20 function in embryonic cardiomyocytes during the early stages of heart chamber formation (Moses et al., 2001). *Nkx2.5Cre;CC-Tbx20* DTG embryos exhibit growth retardation and obvious lethality by E10.5 (Table 1), therefore all the experimental analyses were performed at E9.5. Nkx2.5Cre-mediated overexpression of Tbx20 in embryonic cardiomyocytes results in a smaller heart size in E9.5 DTG embryos (black arrowheads in Fig. 5A, B), compared to littermate control embryos (white arrowheads in Fig. 5A, B). In heart tissue sections of the DTG and the littermate STG control embryos, cardiomyocyte differentiation is apparent by MF20 immunoreactivity (Fig. 5D, G), but the ventricles are thin with decreased trabeculation in *Nkx2.5Cre;CC-Tbx20* embryos at E9.5 (Fig. 5C, F). In addition, endocardial cushion formation seems to be unaffected in E9.5 DTG hearts as evidenced by similar Twist1-antibody reactivity in cushion mesenchymal cells compared to littermate control hearts (Fig. 5E, H). Tbx20 overexpression in DTG embryos was confirmed by increased Tbx20 antibody reactive nuclei in the DTG ventricular myocardium, including LV, RV and OFT regions compared to a littermate control heart (Fig. 5J, L). Direct cell counts reveal that approximately 38.8% MF20-positive cardiomyocytes are also positive for Tbx20, compared to 16% Tbx20 and MF20 positive cardiomyocytes in littermate controls (Fig. 5M). Quantitative Western blot analysis reveals a 3.4-fold overexpression of Tbx20 protein in E9.5 DTG hearts, compared to littermate STG controls (Fig. 5N, O). Thus induced expression of Tbx20 in the primitive heart tube leads to reduced cardiac growth, which is in contrast to the increased cardiac growth observed in the ventricular myocardium of β MHCCre;*CC-Tbx20* DTG embryos at E14.5.

Mice lacking Tbx20 fail to activate chamber lineage maturation genes (Cai et al., 2005; Singh et al., 2005; Stennard et al., 2005). Therefore expression of indicators of chamber differentiation was assessed in the *Nkx2.5Cre;CC-Tbx20* DTG myocardium by ISH. The expression of *Tbx2* is decreased in the E9.5 AVC myocardium overexpressing Tbx20, compared to its normal expression in the littermate control AVC myocardium (Fig. 6A, B). The expression of *Tbx5* is also down-regulated throughout the E9.5 mutant myocardium, compared to its strong expression in the STG control myocardium (Fig. 6C, D). In contrast, expression of *Bmp10* is comparable in the E9.5 DTG mutant heart, compared to its normal expression in the STG littermate control (Fig. 6E, F). Likewise, the expression of chamber differentiation markers *Nppa*, *Smpx*, and *MLC2v* is similar in the DTG and STG embryos (Fig. 6G-L). Gene expression analysis by qRT-PCR confirmed decreased expression of *Tbx5* and unchanged expression of *Bmp10*, *Nppa*, *Smpx* and *Mlc2v* in E9.5 DTG hearts relative to littermate STG controls (Fig. 6M). Together these data demonstrate that the Nkx2.5Cre-mediated overexpression of Tbx20 in embryonic cardiomyocytes results in decreased *Tbx5* expression, but does not affect expression of markers of chamber myocardial maturation.

Nkx2.5Cre-mediated Tbx20 overexpression leads to decreased proliferation with induction of p21^{CIP1} in cardiomyocytes

Cardiomyocyte proliferation and expression of cell cycle regulatory genes was examined in *Nkx2.5Cre;CC-Tbx20* DTG hearts. Co-labeling of pHH3 and MF20 demonstrates reduced cardiomyocyte proliferation in E9.5 DTG embryos, compared to littermate STG controls (Fig. 7A, B). Quantitation of these results demonstrates that 18.5% of MF20 positive cardiomyocyte cell nuclei are also positive for pHH3 in DTG myocardium, compared to 36.6% MF20 and pHH3 positive nuclei in STG controls (Fig. 7C). In contrast, the percent of nuclei with pHH3 immunoreactivity in the endocardial endothelial cell layer is unchanged in DTG versus STG hearts (data not shown). Consistent with reduced cardiomyocyte proliferation, expression of the cyclin dependent kinase (CDK) inhibitor p21^{CIP1} is

increased in DTG myocardium overexpressing Tbx20, compared to the littermate control myocardium as detected by immunostaining and qRT-PCR (Fig. 7D-F, I). Expression of additional cell cycle regulatory genes that promote proliferation, including *cyclin A2*, *cyclin D1*, and *cyclin E1*, also is reduced in *Nkx2.5Cre;CC-Tbx20* as detected by qRT-PCR. However mRNA expression of another CDK inhibitor (CKI), *p27^{KIP1}* remains unchanged in E9.5 DTG hearts compared to controls (Fig. 7I). In contrast to β *MHCCre;CC-Tbx20* DTG hearts, *N-myc1* gene expression is decreased in the E9.5 *Nkx2.5Cre;CC-Tbx20* DTG ventricular myocardium as detected by ISH and qRT-PCR (Fig. 7G-I), consistent with reduced cardiomyocyte proliferation in these embryos.

Tbx20 overexpression inhibits activation of ERK1/2 MAPK in *Nkx2.5Cre;CC-Tbx20* embryonic cardiomyocytes *in vivo*

In order to further characterize the differential effects of Tbx20 on embryonic versus fetal cardiomyocyte proliferation, pERK1/2 expression was evaluated in E9.5 *Nkx2.5Cre;CC-Tbx20* DTG hearts compared to littermate controls by antibody staining (A-D) and Western blot (E-F) analyses. At E9.5, dpERK is normally active in the myocardium and has been implicated as a downstream mediator of Neuregulin signaling (Lai et al., 2010). In *Nkx2.5Cre;CC-Tbx20* DTG hearts, dpERK expression is reduced throughout the ventricular chamber myocardium, compared to control hearts (Fig. 8A-D). Quantitation of these results by Western blot analysis demonstrates that the ratio of dpERK/total ERK expression is reduced by 42% in *Nkx2.5Cre;CC-Tbx20* hearts, relative to control hearts, and that total ERK protein levels are unchanged (Fig. 8E, F). Together, these data indicate that ERK activation is decreased with Tbx20 overexpression at E9.5. However, the expression of *Nrg1*, mRNA predominant in endothelial lineage, is apparently unaffected by Tbx20 overexpression as detected by qRT-PCR and IHC (data not shown). In contrast to the increased expression in *Nkx2.5Cre;CC-Tbx20* DTG hearts, dpERK activation is not decreased in β *MHCCre;CC-Tbx20* ventricular cardiomyocytes, compared to littermate STG controls, consistent with the observed stage-specific effects on cell proliferation (Supplemental Fig. S2E-H). Together, these data demonstrate that increased Tbx20 protein levels inhibit dpERK activation in embryonic (E9.5), but not fetal (17.5), cardiomyocytes *in vivo*.

Discussion

Here we demonstrate that Tbx20 overexpression in the primitive heart results in decreased cardiomyocyte cell proliferation with decreased *N-myc1* expression at E9.5. Previous studies reported that mice with loss of Tbx20 also exhibit reduced cardiomyocyte proliferation and decreased expression of *N-myc1* at E10.5 (Cai et al., 2005; Singh et al., 2005; Stennard et al., 2005). Thus, increased or decreased Tbx20 expression similarly affects cardiomyocyte proliferation and *N-myc1* gene expression during the initial stages of heart chamber maturation. *Nkx2.5Cre*-mediated overexpression of Tbx20 also results in reduced expression of multiple cyclin genes (*A2*, *D1* and *E1*), as well as increased expression of the cell cycle inhibitor *p21^{CIP1}*, consistent with the observed reduction in cardiomyocyte proliferation. Neuregulin signaling has been implicated chamber-specific gene regulation and in ventricular trabeculation through dpERK activation (Lai et al., 2010; Stennard et al., 2005; Woldeyesus et al., 1999). Similar to loss of *Nrg1* function, Tbx20 overexpression leads to decreased dpERK expression and decreased cell proliferation. However, unlike embryos with *Nrg1* or Tbx20 loss-of-function, markers of chamber myocardial maturation are normally induced with Tbx20 overexpression. Thus the level of Tbx20 expression is a critical determinant in cardiomyocyte cell proliferation and lineage maturation in embryonic cardiomyocytes.

In contrast to embryonic cardiomyocytes, β MHCCre-mediated Tbx20 overexpression in fetal ventricular cardiomyocytes (E12.5-E17.5) promotes cell proliferation. Tbx20 overexpression at fetal stages leads to increased expression of *N-myc1*, *Bmp10*, pSmad1/5/8, and *Tbx5*, all of which promote cardiomyocyte cell proliferation (Brown et al., 2005; Cai et al., 2005; Chen et al., 2004; Hatcher et al., 2001). *N-myc1* has been identified as a direct downstream target of Tbx20, and increased Tbx20 binding to T-box responsive elements in the *N-myc1* promoter region is observed in fetal cardiomyocytes, supporting a direct transcriptional activation mechanism (Cai et al., 2005). However, *N-myc1* gene expression is not induced in embryonic cardiomyocytes with Tbx20 overexpression, providing evidence for a more complex regulatory mechanism. Likewise *Bmp10* expression and pSmad1/5/8 activation, required for fetal cardiomyocyte cell proliferation (Chen et al., 2004; Chen et al., 2006), are increased in response to Tbx20 overexpression at fetal, but not embryonic, stages. Tbx5 also promotes cell proliferation in cardiomyocytes, and the observed increase in *Tbx5* expression with Tbx20 overexpression at E14.5, but not E9.5, could contribute to the stage-specific increase in cell proliferation of fetal cardiomyocytes (Brown et al., 2005; Hatcher et al., 2001). Together these analyses demonstrate that embryonic and fetal cardiomyocytes are distinct in their responses to Tbx20 overexpression, which may be indicative of stage-specific differential regulation of cofactors or intersecting signaling pathways. However, further studies are necessary to fully characterize these complex regulatory mechanisms.

Tbx20 has been implicated as both an upstream regulator and downstream target of BMP signaling. Here we demonstrate that Tbx20 overexpression in fetal cardiomyocytes leads to increased *Bmp10* expression and pSmad1/5/8 activation. In addition, *Bmp10* is necessary and sufficient to activate *Tbx20* expression in the fetal myocardium, and a conserved Smad binding site mediates *Bmp10* induction of *Tbx20* proximal promoter sequences in cell culture studies (Zhang et al., 2011). Together, these data provide evidence for a feedforward regulatory mechanism of Tbx20 and *Bmp10* during heart chamber maturation. Likewise, genetic deletion of *Tbx20* specifically from the atrioventricular canal (AVC) myocardium results in downregulation of *Bmp2*, and *Bmp2* induces *Tbx20* expression in endocardial cushion cells supporting a similar feedforward mechanism in endocardial cushion development (Cai et al., 2011; Shelton and Yutzey, 2007). Additional feedback regulatory mechanisms in BMP/Smad signaling occur at the protein level since Tbx20 interacts with Smad1/5 proteins to attenuate their transcriptional regulatory activity (Singh et al., 2009). Together these studies demonstrate that Tbx20 intersects with BMP signaling in multiple ways to regulate diverse aspects of heart formation, including myocardial cell proliferation and endocardial cushion development.

Several T-box transcription factors, including Tbx2, Tbx3, and Tbx5, coordinately regulate connexin gene expression in the CCS, and *Cx40* is a direct downstream target gene of Tbx5 (Aanhaanen et al., 2011; Bakker et al., 2008; Bruneau et al., 2001; Moskowitz et al., 2004). However, Tbx20 function in CCS development has not previously been reported. Tbx20 overexpression in fetal ventricular cardiomyocytes leads to increased expression of *Tbx5*, *Cx40*, and *Cx43* throughout the ventricular myocardium. Since *Cx40* and *Cx43* are regulated by multiple T-box transcription factors, it is likely that increased expression of Tbx20 disrupts the balance of repressive and activating T-box factors on these gene regulatory elements leading to their increased expression in the ventricular myocardium. However the dysregulation of connexin gene expression is apparently insufficient to cause cardiac arrhythmias in adult animals (data not shown). It is striking to note that expression of *Nppa*, which is responsive to Tbx5, Tbx2, and Tbx20, is apparently unaffected by Tbx20 overexpression in fetal ventricular cardiomyocytes (Habets et al., 2002; Plageman and Yutzey, 2004; Stennard and Harvey, 2005). Thus T-box regulation of conduction gene expression is more sensitive to increased Tbx20 than is the expression of chamber myocardium genes, such as *Nppa*, in the fetal myocardium. Together, these results

demonstrate that ventricular cardiomyocytes with increased *Tbx20* expression exhibit enhanced molecular features of the CCS, including increased expression of *Tbx5*, *Cx40* and *Cx43*.

In human patients, *TBX20* gain- and loss-of-function mutations are associated with a wide spectrum of cardiovascular abnormalities, including cardiomyopathies and congenital valvuloseptal defects (Kirk et al., 2007; Posch et al., 2010). Defects in prenatal heart chamber growth can occur in individuals with a *TBX20* loss-of-function mutation, consistent with the importance of *Tbx20* function in cardiac growth during development (Kirk et al. 2007). Gain- and loss-of-function mutations in *TBX20* also are associated with dilated cardiomyopathy in adult and pediatric patients (Kirk et al., 2007; Posch et al., 2010). Arrhythmias and sudden death have been reported in patients with a *TBX20* mutation, and conditional loss of *Tbx20* in adult mice results in severe cardiomyopathy associated with arrhythmias and death (Qian et al., 2008; Shen et al., 2011). Here, we provide evidence that increased levels of *Tbx20* can affect cardiac conduction system gene expression during development, further supporting *TBX20* as a candidate gene in hereditary conduction system anomalies. The combination of human genetic analyses and studies in animal model systems has linked *Tbx20* function to congenital cardiac malformations, conduction system anomalies, and adult cardiomyopathy. Therefore manipulation of *Tbx20* function or intersecting regulatory pathways could be exploited therapeutically. However these studies should proceed with caution because increased or decreased *Tbx20* function in cardiomyocytes can lead to pleiotropic downstream effects on cell proliferation, lineage maturation, or conduction mediated by *Tbx20* and its complex interacting regulatory factors.

Supplementary Material

Refer to Web version on PubMed Central for supplementary material.

Acknowledgments

We thank Joy Lincoln, Christina Alfieri, Jonathan Cheek, and Arunima Sengupta for technical assistance and scientific discussions. We thank Izhak Kehat for help in performing the EKG measurement in adult mice. We thank Dr. Robert J. Schwartz (Texas Heart Institute, University of Houston, Texas) for generously provided us the *Nkx2.5Cre* transgenic mice. We also thank Drs. Weinian Shou (Indiana University School of Medicine, Indianapolis), Vincent M. Christoffels (Heart Failure Research Center, University of Amsterdam, Amsterdam, The Netherlands), Benoit G. Bruneau (Cardiovascular Research Institute and Department of Biochemistry and Biophysics, University of California, San Francisco), and Chen-Leng Cai (Center for Molecular Cardiology & Black Family Stem Cell Institute, Mount Sinai School of Medicine, New York, New York) for their generosity in providing us plasmids for *in-situ* hybridization.

Sources of Funding

This work was supported by an American Heart Association-Great Rivers Affiliate Post-Doctoral Fellowship (0825627D) to SC and NIH/NHLBI R01-HL082716 to KEY.

References

- Aanhaanen WT, Boukens BJ, Sizarov A, Wakker V, de Gier-de Vries C, van Ginneken AC, Moorman AF, Coronel R, Christoffels VM. Defective *Tbx2*-dependent patterning of the atrioventricular canal myocardium causes accessory pathway formation in mice. *J Clin Invest.* 2011; 121:534–544. [PubMed: 21266775]
- Araki K, Araki M, Miyazaki J, Vassalli P. Site-specific recombination of a transgene in fertilized eggs by transient expression of Cre recombinase. *Proc Natl Acad Sci U S A.* 1995; 92:160–164. [PubMed: 7816809]

- Bakker ML, Boukens BJ, Mommersteeg MT, Brons JF, Wakker V, Moorman AF, Christoffels VM. Transcription factor Tbx3 is required for the specification of the atrioventricular conduction system. *Circ Res.* 2008; 102:1340–1349. [PubMed: 18467625]
- Brown DD, Martz SN, Binder O, Goetz SC, Price BMJ, Smith JC, Conlon FL. Tbx5 and Tbx20 act synergistically to control vertebrate heart morphogenesis. *Development.* 2005; 132:553–563. [PubMed: 15634698]
- Bruneau BG, Nemer G, Schmitt JP, Charron F, Robitaille L, Caron S, Conner DA, Gessler M, Nemer M, Seidman CE, Seidman JG. A murine model of Holt-Oram syndrome defines roles of the T-box transcription factor Tbx5 in cardiogenesis and disease. *Cell.* 2001; 106:709–721. [PubMed: 11572777]
- Cai CL, Zhou W, Yang L, Bu L, Qyang Y, Zhang X, Li X, Rosenfeld MG, Chen J, Evans S. T-box genes coordinate regional rates of proliferation and regional specification during cardiogenesis. *Development.* 2005; 132:2475–2487. [PubMed: 15843407]
- Cai X, Nomura-Kitabayashi A, Cai W, Yan J, Christoffels VM, Cai CL. Myocardial Tbx20 regulates early atrioventricular canal formation and endocardial epithelial-mesenchymal transition via Bmp2. *Dev Biol.* 2011; 360:381–390. [PubMed: 21983003]
- Chakraborty S, Cheek J, Sakthivel B, Aronow BJ, Yutzey KE. Shared gene expression profiles in developing heart valves and osteoblast progenitor cells. *Physiol Genomics.* 2008; 35:75, 85. [PubMed: 18612084]
- Chakraborty S, Wirrig EE, Hinton RB, Merrill WH, Spicer DB, Yutzey KE. Twist1 promotes heart valve cell proliferation and extracellular matrix gene expression during development in vivo and is expressed in human diseased aortic valves. *Dev Biol.* 2010; 347:167–179. [PubMed: 20804746]
- Chen H, Shi S, Acosta L, Li W, Lu J, Bao S, Chen Z, Yang Z, Schneider MD, Chien KR, Conway SJ, Yoder MC, Haneline LS, Franco D, Shou W. BMP10 is essential for maintaining cardiac growth during murine cardiogenesis. *Development.* 2004; 131:2219–2231. [PubMed: 15073151]
- Chen H, Yong W, Ren S, Shen W, He Y, Cox KA, Zhu W, Li W, Soonpaa M, Payne RM, Franco D, Field LJ, Rosen V, Wang Y, Shou W. Overexpression of bone morphogenetic protein 10 in myocardium disrupts cardiac postnatal hypertrophic growth. *J Biol Chem.* 2006; 281:27481–27491. [PubMed: 16798733]
- Christoffels VM, Hoogaars WMH, Tessari A, Clout DEW, Moorman AFM, Campione M. T-box transcription factor Tbx2 represses differentiation and formation of the cardiac chambers. *Dev Dyn.* 2004; 229:763–770. [PubMed: 15042700]
- Christoffels VM, Smits GJ, Kispert A, Moorman AF. Development of the pacemaker tissues of the heart. *Circ Res.* 2010; 106:240–254. [PubMed: 20133910]
- Coppen SR, Kaba RA, Halliday D, Dupont E, Skepper JN, Elneil S, Severs NJ. Comparison of connexin expression patterns in the developing mouse heart and human foetal heart. *Mol Cell Biochem.* 2003; 242:121–127. [PubMed: 12619874]
- Davis A, Bradley A. Mutation of N-myc in mice: what does the phenotype tell us? *Bioessays.* 1993; 15:273–275. [PubMed: 8517856]
- Evans-Anderson HJ, Alfieri CM, Yutzey KE. Regulation of cardiomyocyte proliferation and myocardial growth during development by FOXO transcription factors. *Circ Res.* 2008; 102:686–694. [PubMed: 18218983]
- Gurtner A, Fuschi P, Magi F, Colussi C, Gaetano C, Dobbelsstein M, Sacchi A, Piaggio G. NF-Y dependent epigenetic modifications discriminate between proliferating and postmitotic tissue. *PLoS One.* 2008; 3:e2047. [PubMed: 18431504]
- Habets PE, Moorman AF, Clout DE, van Roon MA, Lingbeek M, van Lohuizen M, Campione M, Christoffels VM. Cooperative action of Tbx2 and Nkx2.5 inhibits ANF expression in the atrioventricular canal: implications for cardiac chamber formation. *Genes Dev.* 2002; 16:1234–1246. [PubMed: 12023302]
- Hatcher CJ, Goldstein MM, Mah CS, Delia CS, Basson CT. Identification and localization of TBX5 transcription factor during human cardiac morphogenesis. *Dev Dyn.* 2000; 219:90–95. [PubMed: 10974675]

- Hatcher CJ, Kim MS, Mah CS, Goldstein MM, Wong B, Mikawa T, Basson CT. TBX5 transcription factor regulates cell proliferation during cardiogenesis. *Dev Biol.* 2001; 230:177–188. [PubMed: 11161571]
- Hemmerich P, von Mikecz A, Neumann F, Sozeri O, Wolff-Vorbeck G, Zobelein R, Krawinkel U. Structural and functional properties of ribosomal protein L7 from humans and rodents. *Nucleic Acids Res.* 1993; 21:223–231. [PubMed: 8441630]
- Hinton RB Jr, Lincoln J, Deutsch GH, Osinska H, Manning PB, Benson DW, Yutzey KE. Extracellular matrix remodeling and organization in developing and diseased aortic valves. *Circ Res.* 2006; 98:1431–1438. [PubMed: 16645142]
- Kato T, Kasai A, Mizuno M, Fengyi L, Shintani N, Maeda S, Yokoyama M, Ozaki M, Nawa H. Phenotypic characterization of transgenic mice overexpressing neuregulin-1. *PLoS One.* 2010; 5:e14185. [PubMed: 21151609]
- Kirk EP, Sunde M, Costa MW, Rankin SA, Wolstein O, Castro ML, Butler TL, Hyun C, Guo G, Otway R, Mackay JP, Waddell LB, Cole AD, Hayward C, Keogh A, Macdonald P, Griffiths L, Fatkin D, Sholler GF, Zorn AM, Feneley MP, Winlaw DS, Harvey RP. Mutations in cardiac T-box factor gene TBX20 are associated with diverse cardiac pathologies, including defects of septation and valvulogenesis and cardiomyopathy. *Am J Hum Genet.* 2007; 81:280–291. [PubMed: 17668378]
- Kroger A, Stirnweiss A, Pulverer JE, Klages K, Grashoff M, Reimann J, Hauser H. Tumor suppression by IFN regulatory factor-1 is mediated by transcriptional down-regulation of cyclin D1. *Cancer Res.* 2007; 67:2972–2981. [PubMed: 17409403]
- Lai D, Liu X, Forrai A, Wolstein O, Michalick J, Ahmed I, Garratt AN, Birchmeier C, Zhou M, Hartley L, Robb L, Feneley MP, Fatkin D, Harvey RP. Neuregulin 1 sustains the gene regulatory network in both trabecular and nontrabecular myocardium. *Circ Res.* 2010; 107:715–727. [PubMed: 20651287]
- Lavine KJ, Yu K, White AC, Zhang X, Smith C, Partanen J, Ornitz DM. Endocardial and epicardial derived FGF signals regulate myocardial proliferation and differentiation in vivo. *Dev Cell.* 2005; 8:85–95. [PubMed: 15621532]
- Li P, Cavallero S, Gu Y, Chen TH, Hughes J, Hassan AB, Bruning JC, Pashmforoush M, Sucov HM. IGF signaling directs ventricular cardiomyocyte proliferation during embryonic heart development. *Development.* 2011; 138:1795–1805. [PubMed: 21429986]
- Liberatore CM, Searcy-Schrick RD, Yutzey KE. Ventricular expression of *tbx5* inhibits normal heart chamber development. *Dev Biol.* 2000; 223:169–180. [PubMed: 10864469]
- Lincoln J, Alfieri CM, Yutzey KE. Development of heart valve leaflets and supporting apparatus in chicken and mouse embryos. *Dev Dyn.* 2004; 230:239–250. [PubMed: 15162503]
- Lincoln J, Florer JB, Deutsch GH, Wenstrup RJ, Yutzey KE. ColVa1 and ColXla1 are required for myocardial morphogenesis and heart valve development. *Dev Dyn.* 2006; 235:3295–3305. [PubMed: 17029294]
- Mandel EM, Kaltenbrun E, Callis TE, Zeng XX, Marques SR, Yelon D, Wang DZ, Conlon FL. The BMP pathway acts to directly regulate *Tbx20* in the developing heart. *Development.* 2010; 137:1919–1929. [PubMed: 20460370]
- Moses KA, DeMayo F, Braun RM, Reecy JL, Schwartz RJ. Embryonic expression of an *Nkx2-5/Cre* gene using ROSA26 reporter mice. *Genesis.* 2001; 31:176–180. [PubMed: 11783008]
- Moskowitz IP, Pizard A, Patel VV, Bruneau BG, Kim JB, Kupersmidt S, Roden D, Berul CI, Seidman CE, Seidman JG. The T-Box transcription factor *Tbx5* is required for the patterning and maturation of the murine cardiac conduction system. *Development.* 2004; 131:4107–4116. [PubMed: 15289437]
- Parsons SA, Millay DP, Wilkins BJ, Bueno OF, Tsika GL, Neilson JR, Liberatore CM, Yutzey KE, Crabtree GR, Tsika RW, Molkentin JD. Genetic loss of calcineurin blocks mechanical overload-induced skeletal muscle fiber type switching but not hypertrophy. *J Biol Chem.* 2004; 279:26192–26200. [PubMed: 15082723]
- Plageman TF Jr, Yutzey KE. T-box genes and heart development: putting the “T” in heart. *Dev Dyn.* 2005; 232:11–20. [PubMed: 15580613]

- Plageman TFJ, Yutzey KE. Differential expression and function of Tbx5 and Tbx20 in cardiac development. *J Biol Chem*. 2004; 279:19026–19034. [PubMed: 14978031]
- Posch MG, Gramlich M, Sunde M, Schmitt KR, Lee SH, Richter S, Kersten A, Perrot A, Panek AN, Al Khatib IH, Nemer G, Megarbane A, Dietz R, Stiller B, Berger F, Harvey RP, Ozcelik C. A gain-of-function TBX20 mutation causes congenital atrial septal defects, patent foramen ovale and cardiac valve defects. *J Med Genet*. 2010; 47:230–235. [PubMed: 19762328]
- Qian L, Mohapatra B, Akasaka T, Liu J, Ocorr K, Towbin JA, Bodmer R. Transcription factor neuromancer/TBX20 is required for cardiac function in *Drosophila* with implications for human heart disease. *Proc Natl Acad Sci U S A*. 2008; 105:19833–19838. [PubMed: 19074289]
- Searcy RD, Vincent EB, Liberatore CM, Yutzey KE. A GATA-dependent nkx-2.5 regulatory element activates early cardiac gene expression in transgenic mice. *Development*. 1998; 125:4461–4470. [PubMed: 9778505]
- Sedmera D, Thompson RP. Myocyte proliferation in the developing heart. *Dev Dyn*. 2011; 240:1322–1334. [PubMed: 21538685]
- Sengupta A, Molkentin JD, Paik JH, DePinho RA, Yutzey KE. FoxO transcription factors promote cardiomyocyte survival upon induction of oxidative stress. *J Biol Chem*. 2011; 286:7468–7478. [PubMed: 21159781]
- Shelton EL, Yutzey KE. Tbx20 regulation of endocardial cushion cell proliferation and extracellular matrix gene expression. *Dev Biol*. 2007; 302:376–388. [PubMed: 17064679]
- Shen T, Aneas I, Sakabe N, Dirschinger RJ, Wang G, Smemo S, Westlund JM, Cheng H, Dalton N, Gu Y, Boogerd CJ, Cai CL, Peterson K, Chen J, Nobrega MA, Evans SM. Tbx20 regulates a genetic program essential to adult mouse cardiomyocyte function. *J Clin Invest*. 2011
- Singh MK, Christoffels VM, Dias JM, Trowe MO, Petry M, Schuster-Gossler K, Burger A, Ericson J, Kispiert A. Tbx20 is essential for cardiac chamber differentiation and repression of Tbx2. *Development*. 2005; 132:2697–2707. [PubMed: 15901664]
- Song L, Yan W, Chen X, Deng CX, Wang Q, Jiao K. Myocardial smad4 is essential for cardiogenesis in mouse embryos. *Circ Res*. 2007; 101:277–285. [PubMed: 17585069]
- Stennard FA, Costa MW, Elliott DA, Rankin S, Haast SJ, Lai D, McDonald LP, Niederreither K, Dolle P, Bruneau BG, Zorn AM, Harvey RP. Cardiac T-box factor Tbx20 directly interacts with Nkx2-5, GATA4, and GATA5 in regulation of gene expression in the developing heart. *Dev Biol*. 2003; 262:206–224. [PubMed: 14550786]
- Stennard FA, Costa MW, Lai D, Biben C, Furtado MB, Solloway MJ, McCulley DJ, Leimana C, Preis JI, Dunwoodie SL, Elliot DE, Prall OW, Black BL, Fatkin D, Harvey RP. Murine T-box transcription factor Tbx20 acts as a repressor during heart development, and is essential for adult heart integrity, function and adaptation. *Development*. 2005; 132:2451–2462. [PubMed: 15843414]
- Stennard FA, Harvey RP. T-box transcription factors and their roles in regulatory hierarchies in the developing heart. *Development*. 2005; 132:4897–4910. [PubMed: 16258075]
- Sucov HM, Gu Y, Thomas S, Li P, Pashmforoush M. Epicardial control of myocardial proliferation and morphogenesis. *Pediatr Cardiol*. 2009; 30:617–625. [PubMed: 19277768]
- Takeuchi JK, Mileikovaika M, Koshihara-Takeuchi K, Heidt AB, Mori AD, Arruda EP, Gertsenstein M, Georges R, Davidson L, Mo R, Hui C, Henkelman RM, Nemer M, Black BL, Nagy A, Bruneau BG. Tbx20 dose-dependently regulates transcription factor networks required for mouse heart and motor neuron development. *Development*. 2005; 132:2463–2474. [PubMed: 15843409]
- Takeuchi JK, Ohgi M, Koshihara-Takeuchi K, Shiratori H, Sakaki I, Ogura K, Saijoh Y, Ogura T. Tbx5 specifies the left/right ventricles and ventricular septum position during cardiogenesis. *Development*. 2003; 130:5953–5964. [PubMed: 14573514]
- Woldeyesus MT, Britsch S, Riethmacher D, Xu L, Sonnenberg-Riethmacher E, Abou-Rebyeh F, Harvey R, Caroni P, Birchmeier C. Peripheral nervous system defects in erbB2 mutants following genetic rescue of heart development. *Genes Dev*. 1999; 13:2538–2548. [PubMed: 10521398]
- Xue L, Sun Y, Chiang L, He B, Kang C, Nolla H, Winoto A. Coupling of the cell cycle and apoptotic machineries in developing T cells. *J Biol Chem*. 2010; 285:7556–7565. [PubMed: 20068041]
- Zhang W, Chen H, Wang Y, Yong W, Zhu W, Liu Y, Wagner GR, Payne RM, Field LJ, Xin H, Cai CL, Shou W. Tbx20 transcription factor is a downstream mediator for bone morphogenetic

protein-10 in regulating cardiac ventricular wall development and function. *J Biol Chem.* 2011; 286:36820–36829. [PubMed: 21890625]

Highlights

- Tbx20 promotes cell proliferation and Bmp10/pSmad in fetal ventricular cardiomyocytes.
- Tbx20 promotes cardiac conduction system gene expression in fetal myocardium.
- Tbx20 overexpression inhibits cell proliferation and induces p21 in embryonic cardiomyocytes.
- Tbx20 overexpression inhibits dpERK1/2 activation in embryonic cardiomyocytes.

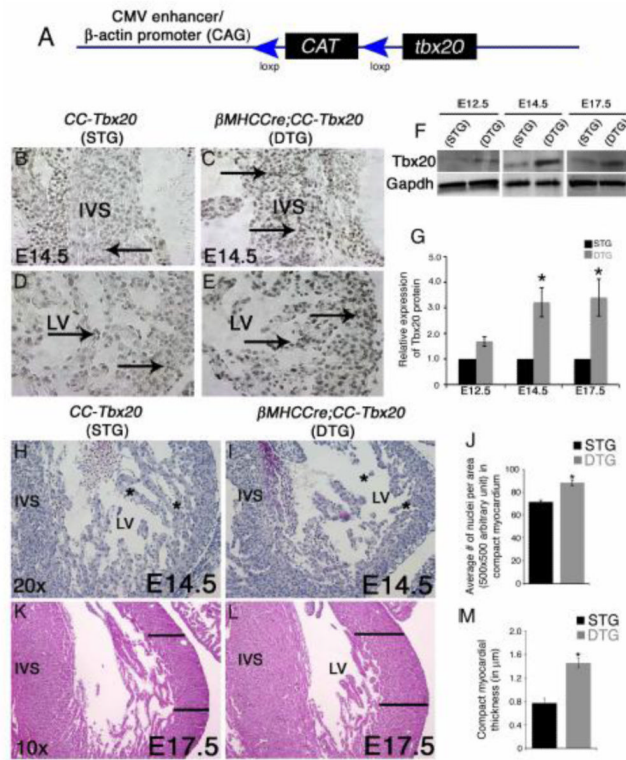


Figure 1. β MHCcre-mediated Tbx20 overexpression in differentiated cardiomyocytes results in thickening of ventricular myocardium

(A) Schematic representation of the *CAG-CAT-Tbx20* (*CC-Tbx20*) transgene for Cre-dependent Tbx20 expression. The *CC-Tbx20* transgene consists of a *CAG* regulatory element (CMV enhancer linked to chicken β -actin promoter) that drives the ubiquitous expression of the *CAT* (chloramphenicol transferase) gene flanked by loxp sites. In the presence of Cre, the *CAT* gene and translational stop sequences are deleted and Tbx20 is expressed. (B-E) Overexpression of Tbx20 in E14.5 chamber myocardium of the β MHCcre;*CC-Tbx20* double transgenic (DTG) animals is detected by Tbx20 antibody reactivity visualized by DAB staining. Increased Tbx20-positive dark brown/black nuclei (arrows) are apparent in the (C) interventricular septum (IVS) and (E) left ventricular (LV) myocardium of a DTG heart compared to a single transgenic (STG) littermate control (B,D). (F, G) Quantitative Western blot analysis reveals a 1.7-fold, 3.2-fold and 3.4-fold increase of Tbx20 protein expression in E12.5, E14.5 and E17.5 DTG hearts, respectively, compared to littermate STG controls. (H-J) In H&E stained sections, decreased trabecular myocardium is apparent in E14.5 DTG LV (compare asterisks in H versus I) and the average number of cells per area of the compact myocardium is increased compared to littermate control (J) ($n = 4$). (K-L) The thickness of the compact myocardium (black lines) is significantly increased in the E17.5 DTG heart as compared to a littermate control in H&E stained sections. (M) The compact layer thickness was quantified ($n = 4$) with statistical significance determined by Student's *t* test, where * denotes $p < 0.05$.

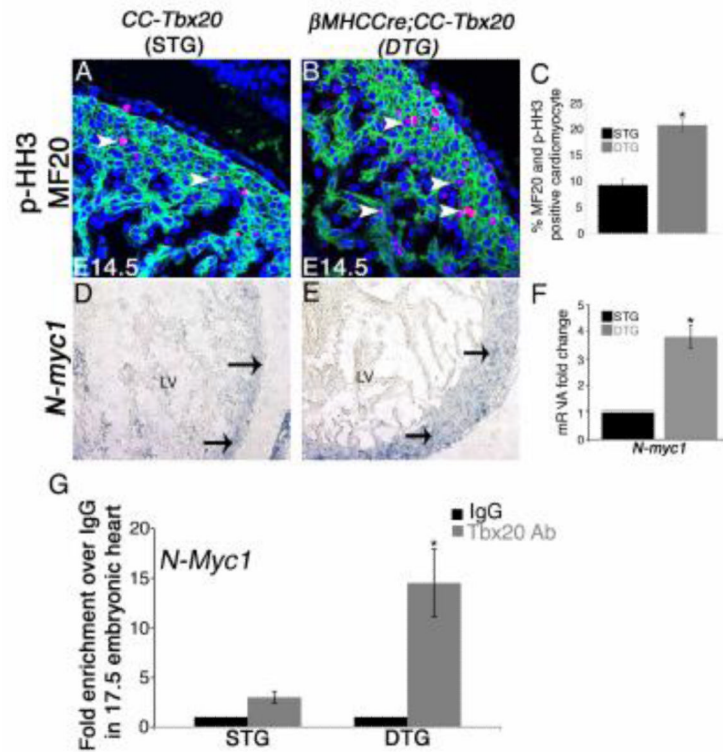


Figure 2. β MHCCre-mediated Tbx20 overexpression promotes cardiomyocyte proliferation with increased binding to the *N-myc1* promoter region in β MHCCre;*CC-Tbx20* fetal hearts *in vivo* (A-B) Cardiomyocyte cell proliferation was detected by phospho-histone H3 (pHH3) nuclear staining in MF20 positive cells at E14.5 in β MHCCre;*CC-Tbx20* (DTG) myocardium (arrowheads in B) compared to littermate controls (arrowheads in A). (C) Quantitation of these results demonstrates a significant increase in proliferative indices of cardiomyocytes overexpressing Tbx20 compared to littermate controls (n = 4). (D-F) Increased expression of *N-myc1*, a known downstream target of Tbx20 in cardiomyocytes, is apparent by ISH in DTG myocardium overexpressing Tbx20 (compare D and E). (F) Observed differences in *N-myc1* gene expression were further confirmed by qRT-PCR analysis of mRNA levels in E14.5 DTG hearts relative to STG controls, set to 1.0 (n = 3). (G) ChIP assays performed at E17.5 demonstrate increased Tbx20 binding (14.5-fold) to a previously identified *T-box* consensus site within intron 1 of the *N-myc1* promoter region in DTG hearts compared to littermate STG controls (3-fold). Graphs represent fold enrichment relative to the IgG antibody control as determined by qPCR (n = 3). Statistical significance was determined by Student's *t* test, where * denotes $p < 0.05$.

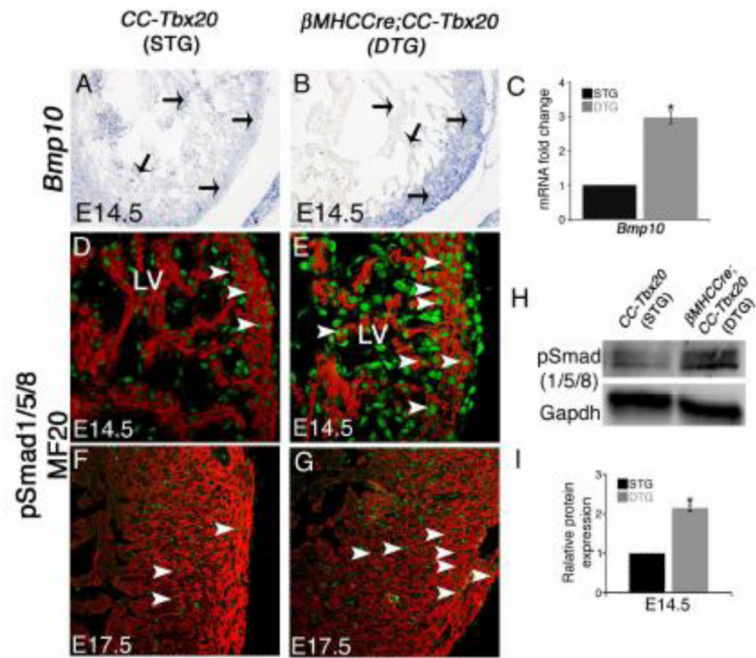


Figure 3. *Bmp10* expression and pSmad1/5/8 signaling are increased in β MHCCre;CC-Tbx20 fetal hearts overexpressing Tbx20

(A-B) Increased expression of *Bmp10* transcripts is detected in the DTG myocardium overexpressing Tbx20 by ISH (arrows in A, B). (C) Observed differences in gene expression was confirmed by qRT-PCR analysis of *Bmp10* mRNA levels in E14.5 DTG hearts relative to levels in STG controls, which were set to 1.0 (n = 3). (D-G) The presence of pSmad1/5/8 was assessed by immunofluorescence and confocal microscopy. pSmad1/5/8 immunoreactivity (green nuclei) is increased in MF20 positive cardiomyocytes (red) and throughout the ventricles overexpressing Tbx20 in both E14.5 (arrowheads in E) and E17.5 (arrowheads in G) DTG hearts, compared to the littermate STG controls (arrowheads in D and F, respectively). (H-I) Quantitation of pSmad1/5/8 protein by Western blot (n = 6) demonstrates a 2.1-fold up-regulation in E14.5 DTG hearts, compared to littermate STG controls. Statistical significance was determined by Student's *t* test, where * denotes $p < 0.05$.

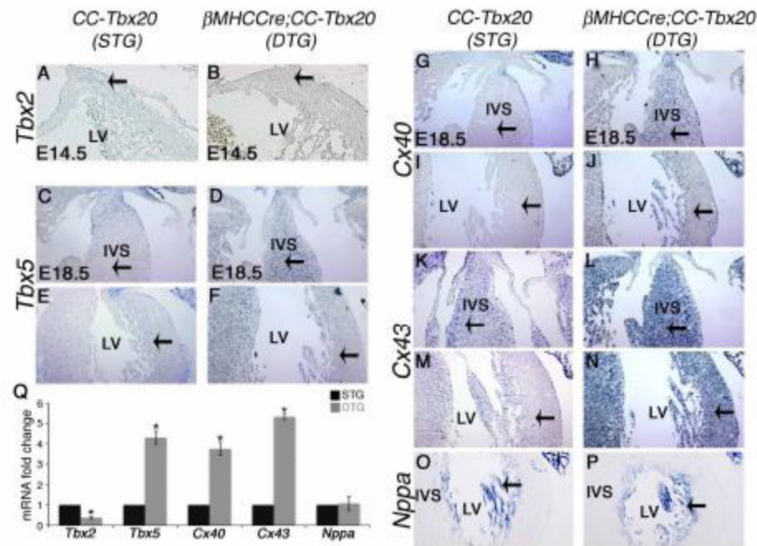


Figure 4. β MHCCre-mediated *Tbx20* overexpression represses *Tbx2*, while inducing expression of *Tbx5*, *connexin40*, and *connexin43* in differentiated cardiomyocytes
 (A-F) Expression of *Tbx2* and *Tbx5* transcripts was evaluated in the β MHCCre;*CC-Tbx20* (DTG) myocardium overexpressing *Tbx20* by ISH. In E14.5 DTG hearts, the expression of *Tbx2* is reduced along the AV canal myocardium (B, arrow) compared a littermate STG control (A, arrow). In E18.5 DTG hearts, *Tbx5* expression is increased throughout the interventricular septum (IVS) and in the ventricles (D, F, arrows) compared to restricted expression in the littermate control heart (C, E, arrows). Expression of *Cx40* (H, J) and *Cx43* (L, N) is increased in the DTG myocardium (arrows) compared to expression in STG littermate controls (G, I and K, M). In contrast, *Nppa* expression is unchanged in the DTG trabecular myocardium compared to the littermate control heart (compare O and P, arrows). (Q) Observed differences in gene expression were further validated by qRT-PCR in DTG hearts relative to STG controls (n = 3). Statistical significance was determined by Student's *t* test, where * denotes $p < 0.05$.

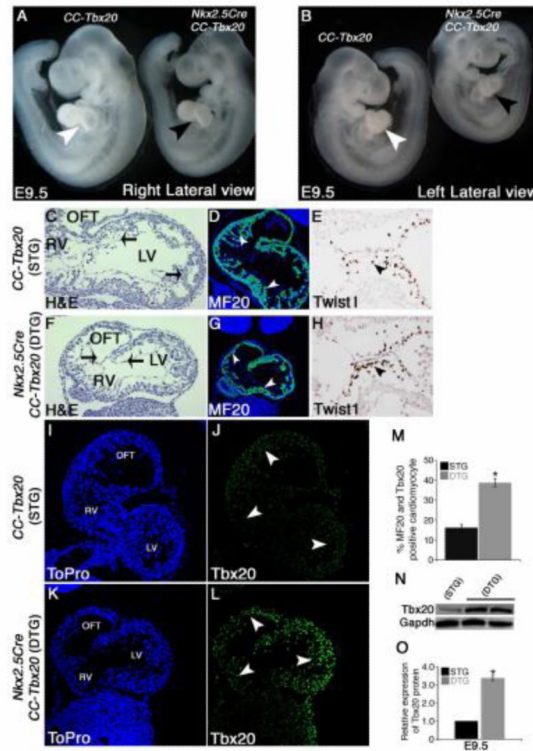


Figure 5. Nkx2.5Cre-mediated Tbx20 overexpression results in a smaller heart with apparently normal endocardial cushion formation

Nkx2.5Cre-mediated overexpression of Tbx20 results in a smaller heart in E9.5 DTG embryos (black arrowheads in A and B) compared to somite-matched STG embryos (white arrowheads in A and B), displayed in both left (A) and right (B) lateral views. Histological (H&E) and MF20 antibody staining also reveal the smaller heart size in *Nkx2.5Cre;CC-Tbx20* (DTG) embryos (compare C versus F and D versus G). The generation of mesenchymal cells and expression of Twist1, indicative of EMT, are apparently normal in the DTG endocardial cushion (arrowhead in H) compared to littermate STG control (arrowhead in E). Tbx20-specific antibody staining reveals Tbx20 overexpression as indicated by positive green nuclei (arrowheads in L), throughout LV, RV and OFT regions of the DTG myocardium compared to the littermate control (arrowheads in J), as detected by immunofluorescence and confocal imaging. (M) Direct cell counts reveal 38.8% of MF20 positive cardiomyocytes are also positive for Tbx20 in DTG ventricular chamber myocardium compared to 16% in littermate controls. (N, O) Quantitative Western blot analysis reveals a 3.4-fold increase of Tbx20 protein expression in E9.5 DTG hearts, compared to littermate STG controls (n = 6-8). Statistical significance is determined by Student's *t* test, where * denotes $p < 0.05$.

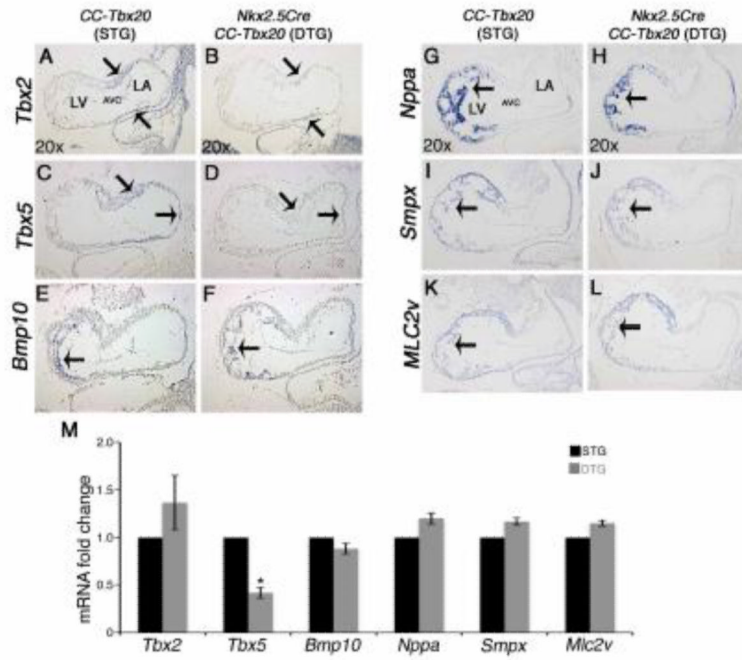


Figure 6. *Nkx2.5*Cre-mediated *Tbx20* overexpression leads to decreased expression of *Tbx5* but normal induction of chamber differentiation markers

Cardiac gene expression was evaluated by ISH. The expression of *Tbx2* is apparently decreased in the AVC myocardium overexpressing *Tbx20* (arrows in B) compared to its normal expression in the littermate control heart (arrows in A). The expression of *Tbx5* (arrows in D) is also decreased throughout the DTG myocardium, compared to littermate control (arrows in C). In contrast, *Bmp10* expression in trabecular cardiomyocytes in the DTG heart is comparable to the littermate control (arrows in E and F). *Nppa* and *Smpx* are expressed in the DTG myocardium overexpressing *Tbx20* (arrows in H and J), as well as in control littermates (arrow in G and I). Likewise the expression of *Mlc2v*, which marks the developing ventricle, is apparent in DTG hearts (arrow in L) and littermate STG controls (arrow in K). (M) Expression of genes analyzed by ISH was quantified in DTG relative to STG hearts by qRT-PCR of RNA isolated at E9.5 ($n = 5$). Statistical significance is determined by Student's *t* test, where * denotes $p < 0.05$.

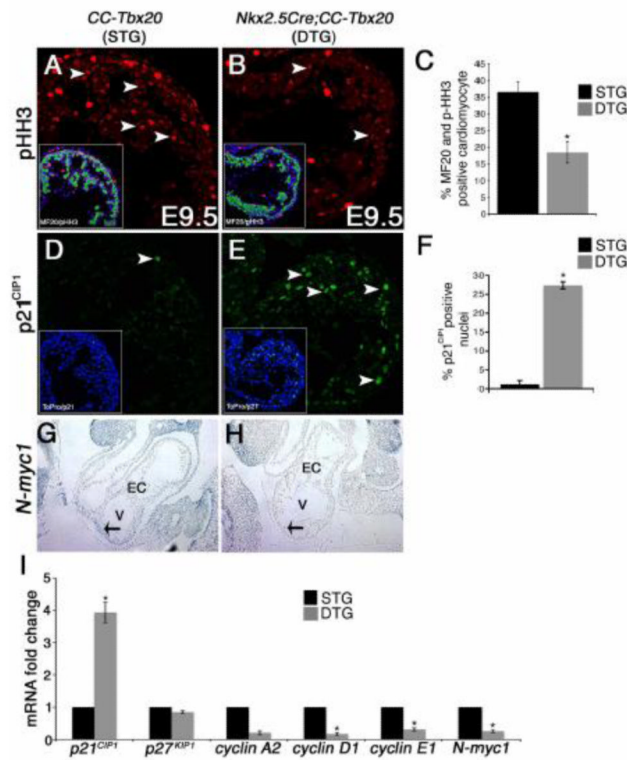


Figure 7. *Nkx2.5Cre*-mediated *Tbx20* expression leads to decreased proliferation with increased expression of *p21^{CIP1}* in cardiomyocytes

(A-C) The number of pHH3 positive cardiomyocyte nuclei in the E9.5 *Nkx2.5Cre;CC-Tbx20* DTG myocardium (arrowheads, B) compared to the littermate control (A) is decreased as visualized by immunofluorescence and confocal microscopy and as quantified in (C) ($n = 4$). Insets in A and B show ventricular chamber myocardium labeled with MF20 and pHH3 antibodies and ToPro3 nuclear counter stain. (D-E) Increased immunostaining of *p21^{CIP1}* (green nuclei) is detected in the DTG myocardium overexpressing *Tbx20* (arrowheads, E) compared to the littermate STG control heart (D) and is quantified in F (1.2% in STG versus 27.3% in DTG). Insets in D and E represent ventricular chamber myocardium labeled with *p21^{CIP1}* antibody and ToPro3. (G-H) *N-myc1* gene expression is decreased in the E9.5 DTG ventricular myocardium overexpressing *Tbx20* (arrow in H), compared to its expression in the littermate control myocardium (arrow in G), as detected by ISH. (I) Expression of cell cycle regulatory genes *p21^{CIP1}*, *p27^{KIP1}*, *cyclin A2*, *cyclin D1*, *cyclin E1*, and *N-myc1* was evaluated in E9.5 DTG hearts by qRT-PCR ($n = 5$). Statistical significance of observed differences was determined by Student's *t* test, where * denotes $p < 0.05$.

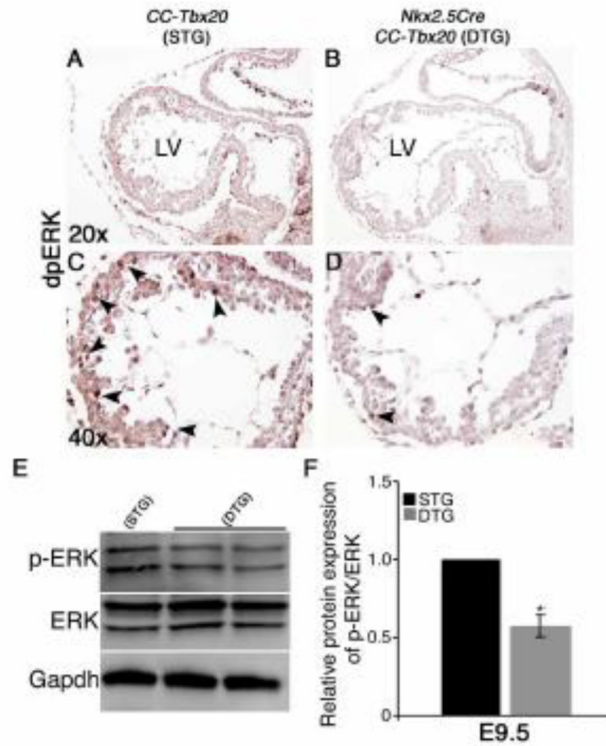


Figure 8. Nkx2.5Cre-mediated overexpression of Tbx20 results in decreased dpERK expression in embryonic cardiomyocytes

(A-D) Expression of the diphosphorylated form of ERK1/ERK2 (dpERK) in E9.5 chamber myocardium is detected by dpERK-specific antibody reactivity visualized by DAB staining. Panels C and D represent higher magnified views (40x objective) of the LV region from panels A and B (20x objective), respectively. Reduced dpERK reactivity (brown/black nuclei) is apparent in the ventricular cardiomyocytes (arrowheads in D) of a DTG embryo compared to the STG littermate control (arrowheads in C). (E-F) dpERK expression was quantified by Western blot analysis as the ratio of dpERK to total ERK protein in E9.5 DTG hearts compared to littermate STG controls (n = 6-8). Statistical significance is determined by Student's *t* test, where * denotes $p < 0.05$.

Table 1

The number and percentage (in parentheses) of wild type (WT), single transgenic (STG), and double transgenic (DTG) individuals obtained from two different crosses at indicated stages of development. The expected Mendelian ratio is indicated in bold and N represents the total number of individuals analyzed for each stage. * denotes dead or partially resorbed embryos.

Stage	N	WT (25%)	STG (50%)	DTG (25%)
<i>Nkx2.5Cre;CC-Tbx20</i>				
E9.5	47	10 (21.3%)	26 (55.3%)	11 (23.4%)
E10.5	54	15 (27.8%)	32 (59.2%)	7 (13%)
E12.5	44	13 (30%)	31 (70%)	0
E14.5	34	14 (41%)	20 (59%)	0
Stage	N	WT (25%)	STG (50%)	DTG (25%)
<i>βMHCCre; CC-Tbx20</i>				
E12.5	35	6 (17.1%)	19 (54.3%)	10 (28.6%)
E14.5	74	14 (19.0%)	40 (54.0%)	20 (27.0%)
E17.5	65	19 (29.2%)	35 (53.8%)	11 (17.0%)
Adult	44	10 (22.7%)	22 (50.0%)	12 (27.3%)